Bone Vol. 26, No. 6
June 2000:603–609

ELSEVIER

Heterogeneity of Bone Lamellar-Level Elastic Moduli

C. E. HOFFLER,[1] K. E. MOORE,[1] K. KOZLOFF,[1] P. K. ZYSSET,[2] M. B. BROWN,[3] and S. A. GOLDSTEIN[1]

[1]*Orthopaedic Research Laboratories, Orthopaedic Surgery, University of Michigan, Ann Arbor, MI, USA*
[2]*Laboratory of Applied Mechanics and Reliability Analysis, Department of Mechanical Engineering, Swiss Federal Institute of Technology, Lausanne, Switzerland*
[3]*Biostatistics Department, School of Public Health, University of Michigan, Ann Arbor, MI, USA*

Advances in our ability to assess fracture risk, predict implant success, and evaluate new therapies for bone metabolic and remodeling disorders depend on our understanding of anatomically specific measures of local tissue mechanical properties near and surrounding bone cells. Using nanoindentation, we have quantified elastic modulus and hardness of human lamellar bone tissue as a function of tissue microstructures and anatomic location. Cortical and trabecular bone specimens were obtained from the femoral neck and diaphysis, distal radius, and fifth lumbar vertebra of ten male subjects (aged 40–85 years). Tissue was tested under moist conditions at room temperature to a maximum depth of 500 nm with a loading rate of 10 nm/sec. Diaphyseal tissue was found to have greater elastic modulus and hardness than metaphyseal tissues for all microstructures, whereas interstitial elastic modulus and hardness did not differ significantly between metaphyses. Trabecular bone varied across locations, with the femoral neck having greater lamellar-level elastic modulus and hardness than the distal radius, which had greater properties than the fifth lumbar vertebra. Osteonal, interstitial, and primary lamellar tissues of compact bone had greater elastic moduli and hardnesses than trabecular bone when comparing within an anatomic location. Only femoral neck interstitial tissue had a greater elastic modulus than its osteonal counterpart, which suggests that microstructural distinctions can vary with anatomical location and may reflect differences in the average tissue age of cortical bone or mineral and collagen organization. (Bone 26: 603–609; 2000)

Key Words: Bone; Mechanical properties; Elasticity; Hardness; Lamellae; Nanoindentation.

Introduction

Advances in our ability to assess fracture risk, predict implant success, and evaluate new therapies for bone metabolic and remodeling disorders demand anatomically specific measures of the local mechanical environment of the cell. Moreover, quantifying anatomic heterogeneity in extracellular matrix properties may provide input for computational models of physiological strategies for balancing mechanical function with mineral homeostasis requirements.

In support of this structure–function paradigm, several investigators have explored regional and anatomical variation in the macroscopic mechanical properties of human cortical and trabecular bone.[2,9,12,16,19,23,24,28,45,49,50,60] Many of these studies have also been summarized in reviews by Reilly and Burstein,[46] Goldstein,[27] and Keaveny and Hayes.[36] Paralleling studies of bone mechanical heterogeneity, investigators have also quantified the biochemical constituency of bone, suggesting that tissue-level variations in intrinsic material properties may exist between lamellae,[34] between cortical and trabecular tissue,[41] and across anatomical locations.[1,29,43] However, the ability of microscopic material properties, when coupled with architecture, microstructure, biochemical composition, and organization, to influence whole bone mechanical integrity is unknown.[13,20,27,31,36]

Although anatomical variations in cortical and trabecular bone material properties have been extensively quantified at the continuum level, parallel studies at the microscopic level are far less numerous. This disparity exists despite the existence of methods to measure microscopic bone tissue properties including microhardness, microtesting, and acoustic techniques.[3,10,15,17,18,32,35,39,42,48,54–56,58,60] Indeed, the study by Weaver[60] stands as the only investigation using a microscopic technique to explicitly characterize bone tissue lamellae from several different organs. Traditionally, hardness is described as the resistance to plastic deformation and is defined as the applied load divided by the residual indentation area.[11] Microscopic hardness correlates with tissue-level elastic modulus in bone,[21,25,32] but it is not a fundamental material property. Hardness integrates all constitutive behaviors of a material exhibited during deformation, making interpretation of its physical meaning challenging.

Recently, investigators have begun to use nanoindentation to measure lamellar-level bone elastic properties.[33,38,51,53,59,63] With 0.3 μN load, 0.16 nm displacement, and 400 nm spatial resolution, nanoindentation has recently been validated as an accurate and reproducible technique for evaluating the elastic moduli of bone tissue lamellae.[33] Unfortunately, a comprehensive evaluation of the lamellar-level elastic properties of bone tissue from different anatomic sites remains unavailable. Hence, the objective of this study was to quantify the elastic properties of human bone tissue lamellae from four different anatomical locations representing different inherent microstructural organization.

Address for correspondence and reprints: Steven A. Goldstein, PhD, Orthopaedic Research Laboratories, University of Michigan, G-0161 400 North Ingalls, Ann Arbor, MI 48109-0486. E-mail: stevegld@umich.edu

8756-3282/00/$20.00
PII S8756-3282(00)00268-4

Bone Vol. 26, No. 6
June 2000:603–609

Materials and Methods

Subjects were obtained through the University of Michigan Anatomical Donations Program. All cadavers were fresh-frozen and screened for arthroplasty, osteosarcoma, paralysis, and metabolic bone disorders, using medical records. Cadavers of uncertain medical history were not included. Osteoporotic specimens were excluded on the basis of femoral neck fractures identified during dissection or radiographically apparent compression fractures in the fourth or fifth lumbar vertebrae. Cortical and trabecular bone specimens were obtained from 10 male subjects (9 white, 1 black) between 40 and 85 years of age. We decided to study the femoral neck and diaphysis, distal radius, and fifth lumbar vertebra for the dual purpose of comparing them with previous investigations and evaluating regions of elevated fracture incidence often associated with bone fragility.[20,40]

All tissue preparations followed previously validated protocols.[33] In the distal radius, bone was sectioned transverse to the long axis immediately proximal to the ulnar articulating surface using an irrigated diamond wafering blade (Buehler Ltd., Lake Bluff, IL). A scalpel was used to remove a 1 cm^2 sample from the palmar surface of 2.8-mm-thick cross sections. The femoral neck was sectioned with an irrigated diamond band saw (Exakt Instruments, Oklahoma City, OK) transverse to its anatomical axis, beginning proximal to the greater trochanter. Sections were made parallel to the plane defined by the portions of the greater and lesser trochanters located closest to the femoral head. One-centimeter-square samples were removed from the lateral portion of the section with a scalpel. In both the distal radius and femoral neck, tissue samples had a trabecular interior bordered on one edge by a compact bone cortex. In the femoral diaphysis, the linea aspera (posterior) was isolated from a 3 in. length axial segment. Transverse sectioning was performed with a diamond wafering blade.

Before sectioning, fifth lumbar vertebrae were screened for compression fractures by comparing their heights with other vertebrae in the subject's spine using anterior-posterior and lateral radiographs. The intervertebral disks, soft tissues, and posterior elements were removed. A diamond band saw irrigated with distilled water was used to section the vertebrae transverse to the spinal axis and immediately cranial to the caudal bony end plate. One-centimeter-square samples containing cortex and internal trabeculae were isolated from the anterior portion of the section with a scalpel.

All specimen sections were about 3 mm thick less the blade thickness (200 μm). All tissue samples were embedded in a weakly exothermic epoxy (PL-1; Photoelastic Division, Measurements Group, Raleigh, NC) which penetrated trabecular pores but not the tissue itself. Previous experiments have demonstrated that the embedding procedure does not effect nanoindentation measurements.[30] Subsequently, tissue samples were secured to polycarbonate platens and surface polished using progressive grades of SiC paper. Specimens were finished with a 0.25 μm diamond slurry and cleansed in an ultrasonic water bath for 15 min. Cranial surfaces were presented for indentation testing.

The NanoIndenter II system (Nano Instruments, Oak Ridge, TN) was used to measure the elastic modulus at the lamellar level of hierarchy. Nanoindentation is the most recent advance in depth-sensing indentation technology. Similar to traditional hardness instrumentation, a diamond probe is pressed into a test material and retracted, leaving a permanent impression. Load and depth are recorded with 0.3 μN and 0.16 nm resolutions, respectively. Doerner and Nix[22] adapted Sneddon's[57] solution to indentation of an elastic half space by a rigid, axisymmetric, flat indenter, and modeled nanoindentation as a deformable cylinder indenting an elastic half space. Assuming a Poisson ratio, isotropic elasticity, rate independent plasticity, and continued contact during initial unloading, Doerner and Nix related the initial unloading stiffness to elastic modulus.[22] Oliver and Pharr[44] refined this approach to accommodate nonlinear unloading behavior due to the varying cross section of the indenter. They also incorporated King's[37] modifications for indenters of varying cross sections. The initial unloading stiffness, S, is related to the elastic modulus as follows:

$$S = \frac{dP}{dh} = 2\beta E_r \sqrt{\frac{A_c}{\pi}} \tag{1}$$

where P = the load, h = the depth, and dP/dh = the initial slope during unloading of the force–displacement curve. β = an empirical factor to distinguish different indenter shapes, and A_c = the projected area of elastic contact. E_r = the reduced modulus and it accounts for the nonrigid indenters.

$$\frac{1}{E_r} = \frac{1 - \nu_b^2}{E_b} + \frac{1 - \nu_i^2}{E_i} \tag{2}$$

E_b and ν_b = the elastic modulus and Poisson ration for bone. E_i and ν_i = the same quantities for the indenter. The projected area of contact, A_c (equation [1]) is determined by the contact depth and is calculated based on the area-to-depth function of the indenter. Recognizing that indenter tip geometry can vary significantly, cross-sectional area as a function of depth is derived empirically for each tip. The experimental model for nanoindentation and the tip shape calibration have been studied extensively and proven to be accurate for aluminum, quartz, sapphire, fused silica, soda lime glass, and tungsten.[44] Recent studies by Rho et al.,[50] Zysset et al.,[63] and Turner et al.[59] have shown that nanoindentation yields reproducible results in bone at the lamellar level.

Hardness is defined as the maximum force divided by the projected area of contact, and may also be computed from the load-displacement data and the area-to-depth function.

$$H = \frac{P_{\max}}{A_c} \tag{3}$$

The NanoIndenter II is equipped with a pyramidal Berkovich diamond indenter, a microscope, and a coordinate table, all located on a vibration isolation platform within a protective cabinet. Load and depth are controlled with an inductive load cell and a capacitive displacement gauge, respectively. Custom irrigation was designed to maintain tissue moisture and included a precautionary solution of 0.5 μg/mL gentamicin (antibacterial) (Life Technologies, Grand Island, NY) to prevent tissue degradation, as testing may extend several hours (**Figure 1**). Indentor tip calibrations were performed before testing.

Using the light microscope, we selected indentation locations based on microstructure. In the distal radius, microstructures were classified as osteonal, interstitial, trabecular, and primary lamellar (**Figure 2**). Femoral neck tissue was separated into osteonal, interstitial, and trabecular microstructures. In the femoral diaphysis, only osteonal and interstitial tissues were present. Osteonal and interstitial tissue regions were selected in spatially adjacent pairs. Trabecular, cortical lamellar, and enthesophytic microstructures were observed in vertebral specimens (**Figure 3**). The thin cortical shell of the vertebrae was noticeably and expectedly devoid of Haversian structures. The circumferential lamellar tissue of the cortex appeared similar to trabecular tissue in architecture but lacked trabecular packets. The enthesophytic tissue was nonlamellar tissue (in transverse sections) localized to the ligamentous-osseous transition known as the enthesis. Often

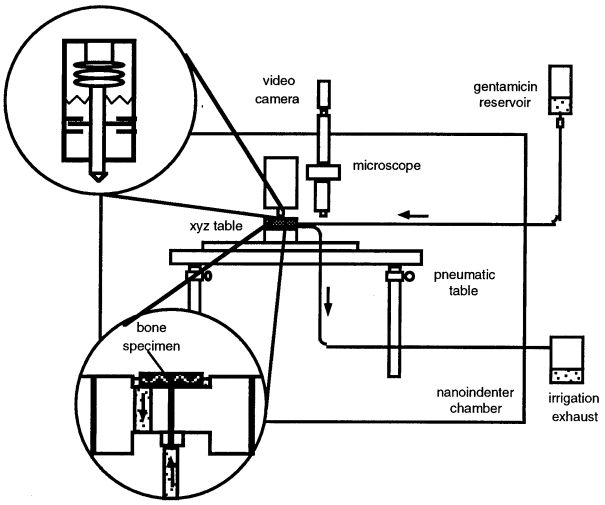

Figure 1. Schematic of Nano Indenter II and custom irrigation system.

called osteophytes, enthesophytes of the anterior vertebral body are hypothesized to result from abnormal ligamentous tractions.[47]

Within a single specimen, nine regions of each microstructure present were tested. At each region of interest, a 30 μm^2 array of four indents was made (totaling 36 indents/microstructure per specimen). Indentation was performed at 10 nm/sec to a maximum depth of 500 nm. Tissue was preconditioned with two preliminary cycles to 100 and 250 nm of depth. As described above, the lamellar-level tissue elastic modulus was then calculated from the unloading segment of the force–displacement curve assuming a Poisson ratio of 0.3. Recent results demonstrate that trabecular tissue may have an isotropic Poisson ratio of 0.25[62] and that lamellar-level elastic modulus varies only within 10% between Poisson ratios of 0.2 and 0.4 when measured with nanoindentation.[63] Lamellar tissue hardness was also determined.

All data were log-transformed to correct for positive skewness. A mixed-model analysis of variance (ANOVA) was performed using SAS 6.11 (SAS Institute, Cary, NC). Bone and microstructure were treated as fixed effects, whereas region and indent number (within the array of four) were treated as random. The subject variable was also considered a random effect. A mixed-model ANOVA is equivalent to a repeated-measures ANOVA when all data values are present, but it is also able to analyze data when some values are missing. A Tukey's multiple range test followed the ANOVA, and significance was attributed to p values <0.05.

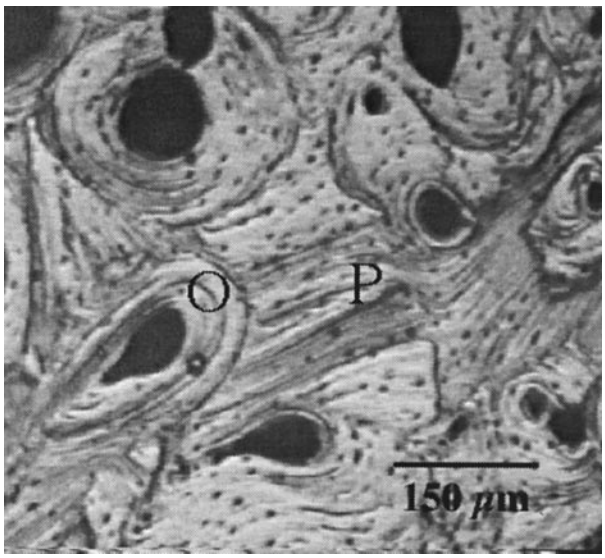

Figure 2. Transverse section of the palmer distal radius cortex detailing osteonal (O) and primary lamellae (P). Original magnification ×200.

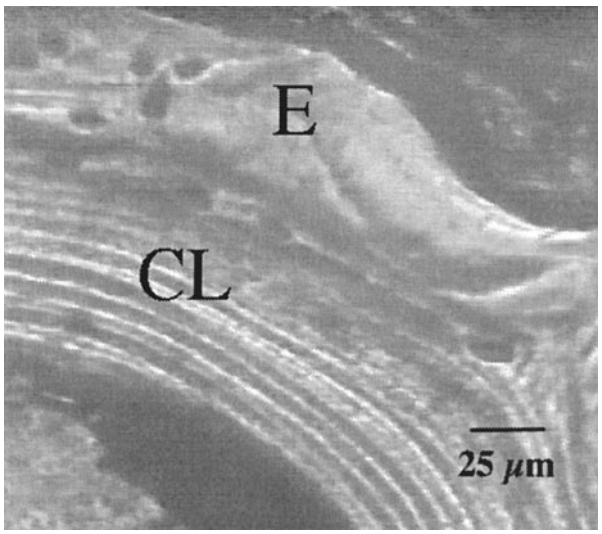

Figure 3. Transverse section of the fifth lumbar vertebral body detailing circumferential lamellae of the cortex (CL) and enthesophytic tissue (EE). Anterior cortex is at the top. Original magnification ×800.

Results

Before statistical analysis, data with zero values were eliminated because they represented errors caused by excess fluid, which impairs sample surface detection. A total of 4037 nonzero observations were made for ten subjects in four anatomic locations. Next, 133 data points were excluded because data were recorded at depths more than 10% away from the 500 nm target depth. Histograms and univariate descriptions were generated for this reduced data set, and 22 statistical outliers were removed. The final data set for analysis contained 3882 observations.

Figure 4 illustrates the heterogeneity in elastic modulus and hardness between anatomic locations for corresponding microstructures. The corresponding statistical results are detailed in **Table 1**. For example, osteonal and interstitial tissue in the femoral diaphysis had significantly greater moduli and hardnesses than corresponding microstructures in the femoral neck and distal radius. Osteonal tissue in femoral neck had an equivalent elastic modulus but lower hardness compared with the distal radius. Interstitial tissues in these two locations had equivalent properties. Trabecular tissue elastic modulus and hardness were all significantly different, with the distal radius having the greatest properties and the vertebra the lowest. Primary lamellar-level bone was also significantly greater in the distal radius compared with the vertebrae in both elastic modulus and hardness.

Differences between microstructural elastic moduli and hardness within an anatomical location are depicted in **Figure 5** and the associated statistical results are shown in **Table 2**. In the femoral diaphysis, the elastic moduli of osteonal and interstitial tissue were not found to be significantly different. However,

Bone Vol. 26, No. 6
June 2000:603–609

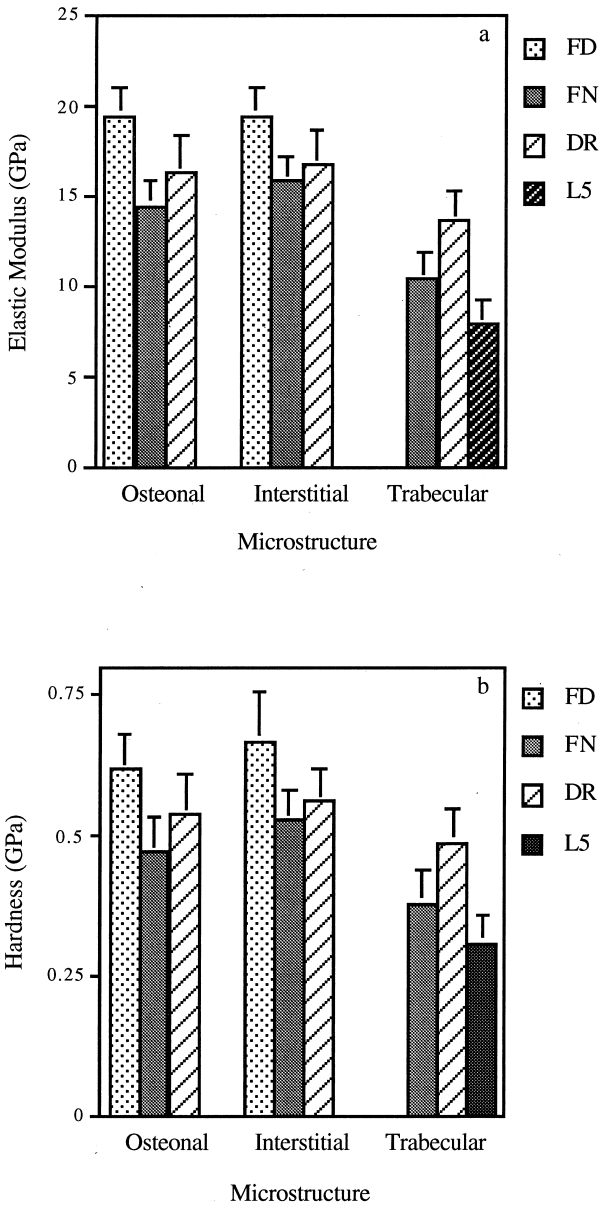

Figure 4. Variations in elastic modulus (a) and hardness (b) between corresponding tissue microstructures in different anatomical locations. Error bars indicate standard errors. FD, femoral diaphysis; FN, femoral neck; DR, distal radius; L5, fifth lumbar vertebra.

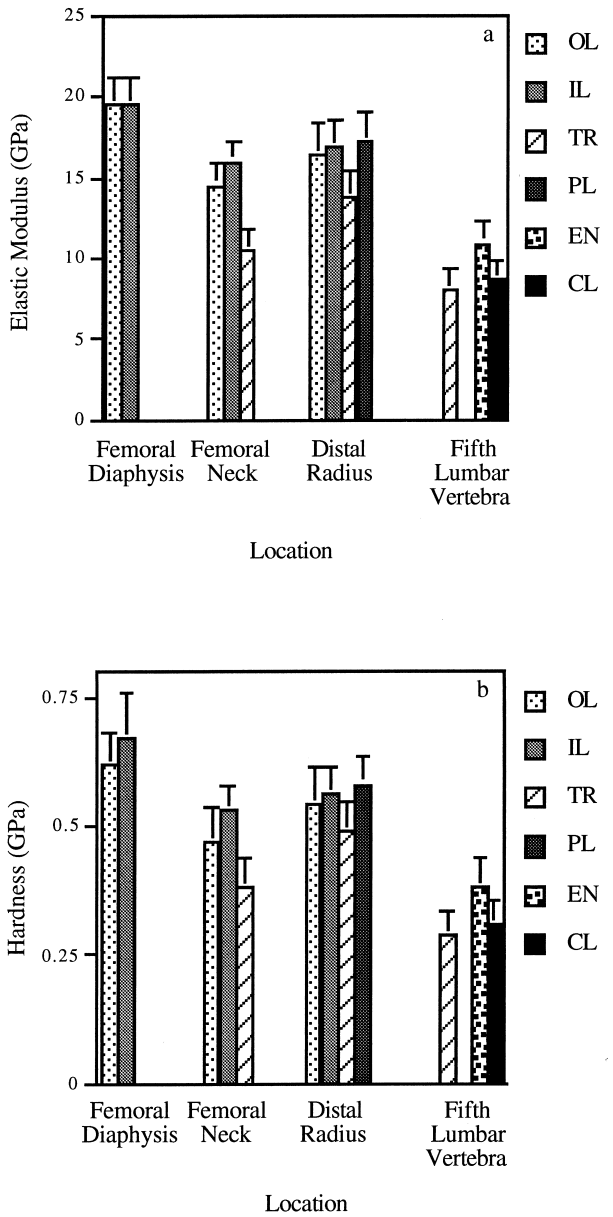

Figure 5. Variations in elastic modulus (a) and hardness (b) between tissue microstructures in the same anatomical location. Error bars indicate standard errors. OL, osteonal; IL, interstitial, TR, trabecular; PL, primary lamellar; EN, enthesophytic; CL, circumferential lamellar.

interstitial hardness was found to be higher than osteonal. Comparisons of femoral neck elastic modulus and hardness values were identical, with interstitial being greater than osteonal, which was greater still than trabecular. Considering vertebral results, trabecular tissue and the circumferential lamellar-level tissue of the cortex were not different. Both had lower properties than the enthesophytic tissue.

In the distal radius, osteonal, interstitial, and primary lamellar-level microstructures did not differ significantly in elastic modulus, and all three values were greater than in trabecular tissue. Hardness results were different, with primary lamellar-level tissue being significantly greater than osteonal and trabecular values. Interstitial hardness was significantly greater than trabecular tissue.

Table 1. Statistical comparisons between corresponding tissue microstructures in different anatomical locations[a]

Microstructure	Elastic modulus	Hardness
Osteonal	FD > FN = DR	FD > DR > FN
Interstitial	FD > FN = DR	FD > FN = DR
Trabecular	DR > FN > L5	DR > FN > L5

KEY: FD, femoral diaphysis; FN, femoral neck; DR, distal radius; L5, fifth lumbar vertebra.
[a]Significance = $p < 0.05$.

Table 2. Summary of statistical comparisons of differences between tissue microstructures in the same anatomical location[a]

Location	Elastic modulus	Hardness
Femoral diaphysis	OL = IL	IL > OL
Femoral neck	IL > OL > TR	IL > OL > TR
Distal radius	OL = IL = PL > TR	PL > OL; PL = IL > TR
Fifth lumbar vertebra	EN > TR = CL	EN > TR = CL

KEY: OL, osteonal; IL, interstitial; TR, trabecular; PL, primary lamellar; EN, enthesophytic; CL, circumferential lamellar.
[a]Significance = $p < 0.05$.

Discussion

Early studies by Weaver determined that the microhardness of interstitial lamellar-level bone is lower in the iliac crest cortex than in diaphyseal cortices.[60] However, interstitial tissue from long bone diaphyses was uniform. Similarly, the present study found diaphyseal tissue to have greater elastic modulus and hardness than metaphyseal tissues for all microstructures. Analogous to the study by Weaver, interstitial tissue properties did not differ significantly between metaphyses. Osteonal elastic moduli also did not differ, but osteonal hardness values were greater in the distal radius than in the femoral neck. Although the data from these studies suggest that interstitial bone from similar sites has comparable properties, these results must be treated with caution. Specifically, Weaver reported data based on the three highest hardness values from a sample of ten. This protocol likely skewed his data toward comparisons between the oldest (longest time passed since deposition) tissue elements, and may not be reflective of the average interstitial tissue properties.[60]

Several other distinctions were found between corresponding microstructures in different locations. An interesting result was that trabecular tissue lamellar-level properties varied between anatomical locations. Specifically, the femoral neck had greater elastic modulus and hardness than the distal radius, which had greater properties than the fifth lumbar vertebra. An important implication of these data is that tissue-quality characterizations extrapolated from one site to another may be erroneous. Similar heterogeneity has been demonstrated for trabecular bone material properties[19,28] and architecture[19] at larger scales of organization.

Mineral content has been shown to correlate with bone lamellar-level microhardness.[3,15,21,25,32,60] We believe that the heterogeneity of bone lamellar-level elastic and hardness properties is likely related to the mineral, collagenous, and noncollagenous protein composition. Moreover, these differences in constituency likely reflect differential metabolic demands, which may influence the process of remodeling. Quantitative measures of mineral and protein concentration at resolutions comparable to nanoindentation are needed to confirm these postulates. In addition, mineral and collagen organization may contribute to anatomical location differences observed at the lamellar level.[3,25,60,61]

Femoral neck trabeculae have the greatest lamellar-level elastic modulus and hardness compared with the distal radius and fifth lumbar vertebra (males aged 40–85 years); yet, lifetime fracture risk for males over age 50 is greatest in the proximal femur.[40] Therefore, lamellar-level elastic modulus and hardness may not explain whole bone fracture patterns. Lamellar elastic modulus and hardness are related to elastic (reversible) and plastic flow properties, respectively, and may not be critical to whole bone fracture resistance. Ultimate, fatigue, and fracture toughness properties should also be explored. Alternatively, trabecular architecture or environmental factors may be more sensitive determinants of fracture risk.

Differences between microstructures within anatomical locations were also noted. Osteonal, interstitial, and primary lamellar tissues, the elements of compact bone, had greater elastic moduli and hardnesses than trabecular bone. The lower properties of trabecular bone likely reflect elevated rates of bone turnover and coincidental decreased mineral content. Cortical bone elastic modulus values ranged from 19.47 ± 1.63 GPa (mean ± standard error) in the femoral diaphysis to 14.53 ± 1.41 GPa in the femoral neck. Trabecular tissue had their highest lamellar-level modulus values in the distal radius (13.75 ± 1.67 GPa) and their lowest in the vertebrae (8.02 ± 1.31 GPa). We tested trabeculae along several geometric axes; cortical bone microstructures were tested in the longitudinal direction. Variation exists in collagen fiber orientations in both cortical and trabecular bone measurements. Specifically, osteonal bone measurements represent a random mixture of osteons, with collagen fibers preferentially oriented longitudinally, transversely, or alternating.[4–8] Owing to the complex architecture of trabecular bone, measurements in trabecular lamellar tissue were also made at varying orientations with regard to collagen orientation. The effect of different distributions of collagen fiber orientation within microstructural groups is unknown and may be ascertained in future studies.

Many investigators have concluded that cortical bone tissue elastic moduli are greater than trabecular tissue using microtesting techniques.[17,18,39,48] Those studies were limited by the unquantified interaction of porosity, microarchitecture, and lamellar-level material properties in defining microspecimen mechanical properties. The micron resolution of nanoindentation allowed us to test mechanical properties at a scale independent of microstructural influences. Our results provide lamellar-level evidence that the elastic properties of cortical bone are greater than trabecular bone under moist conditions. Rho et al. published similar data on dry bone, but not within the same anatomical site.[51]

Mbuyi-Muamba and Dequeker compared cortical and trabecular tissues from matched sites and discovered trabecular mineral to be much more extractable, whereas the collagen-to-sialoprotein ratio was consistently higher in cortical bone.[41] Osteopontin and bone sialoprotein have been implicated in the processes of mineralization, cell adhesion, and resorption.[14,52] Hence, these discrepancies likely reflect the distinct metabolic and mechanical functions of cortical and trabecular bone, and may be responsible for observed differences in lamellar-level mechanical properties.

In contrast to recent findings,[51,63] interstitial bone did not always have greater properties than osteonal tissue. Only the femoral neck interstitial tissue had a greater elastic modulus than its osteonal counterpart. Elastic moduli of osteonal and interstitial microstructures in the femoral diaphysis and distal radius were indistinguishable. These data suggest that the distinction between microstructures can vary with anatomical location. The discrepancy may result from differences in the average tissue age of the three cortical bone locations. Older average tissue ages in

Bone Vol. 26, No. 6
June 2000:603–609

the femoral diaphysis and distal radius would lead to more mineralized tissue elements. If remodeling has declined in these tissues, the newest osteons may in fact be old in absolute time, and also heavily mineralized. If few young osteons are present, the average difference in osteonal and interstitial tissue elastic moduli may become negligible. The femoral neck may have a lower average tissue age and therefore exhibit a more pronounced separation between osteonal and interstitial tissue elastic modulus values. Again, quantitative measures of mineral and protein concentration at resolutions comparable to nanoindentation are needed to address these hypotheses.

Interestingly, comparisons between microstructures differ when one examines hardness values. Interstitial tissue hardness is greater than osteonal in the femoral neck and diaphysis, but the two microstructures are equal in the distal radius. Whereas microscopic hardness has been demonstrated to correlate with tissue elastic modulus,[21,25,32] these results emphasize that elastic modulus and hardness are both conceptually and physically distinct. Elastic modulus characterizes rate-independent reversible material behavior, but hardness describes resistance to plastic deformation. Alternatively, one may assert that the discrepancy stems from inherent inaccuracies in the indentation technique for heterogeneous materials, but currently there are no data to support this hypothesis.

A new finding from this study is that primary lamellar bone is indistinguishable from interstitial bone in lamellar-level elastic modulus and hardness in the distal radius. Its elastic modulus is also equivalent to osteonal tissue, but its hardness is greater. This suggests that primary lamellar bone and Haversian bone are mechanically similar and differ only morphologically.

We have also demonstrated that the circumferential lamellar tissue of the fifth lumbar vertebra cortex is not different from trabecular tissue in lamellar-level elastic modulus and hardness. This observation suggests that vertebral body properties are reflective of its trabecular tissue compartment, without the support of a Haversian bone cortex. Rho reported an elastic modulus of 13.5 ± 2.0 GPa for dry thoracic vertebrae trabeculae,[51] which is much higher than the values found for moist lumbar vertebrae circumferential and trabecular lamellar tissues (8.02 ± 1.31 and 8.57 ± 1.25 GPa, respectively) in the current study. The large discrepancy likely reflects the absence of tissue moisture and possibly anatomical location variation.[33]

The elastic properties of the vertebral body enthesophytes were found to be substantially greater in elastic modulus and hardness than the surrounding trabecular lamellar tissue. Enthesophytes are hypothesized to result from abnormal ligamentous tractions, i.e., a perturbed mechanical environment. Our data may represent the first quantification of an extracellular matrix–level material adaptation to an altered mechanical environment in this region.

Regarding nanoindentation technique, microscale tissue is modeled using isotropy and rate independent plasticity; yet, tissue-level viscoplasticity[26] and ultrastructural anisotropy have been well documented.[3,60,61] Although these model assumptions may distort nanoindentation measures, consistent application of experimental protocols still allows one to make quantitative comparisons at the lamellar level.[51,59,63]

The primary limitation in this study was its modest sample, which was not diverse with respect to gender or race. It is possible that anatomical variations in lamellar elastic modulus or hardness are different in women. Also, bone density may differ between races, so calculations were made using only the nine white subjects. Calculations with the nine white subjects alone did not indicate that the data for the black subject was sufficiently different to be considered outliers.

The absolute property values produced by this study may not reflect the larger population, but the presence of microscopic anatomical variation is clear. Only elastic modulus and hardness were measured. Other material properties such as fatigue and impact resistance may exhibit different variations. The relative importance of different lamellar-level material properties in specifying bone tissue integrity is unknown.

Because the material properties of microscopic lamellar bone are not homogeneous, bone architecture and mass are not the sole determinants of skeletal mechanical competence. Hierarchical studies of microscopic material properties, ultrastructural organization, architecture, and mass, all on the same tissue sample, are necessary to define the relative contributions of these properties to bone tissue integrity. Coordinated mechanical, biochemical, and metabolic characterizations may also further our understanding of the balance between mechanical and homeostatic functions.

Acknowledgments: The authors recognize the contributions of W. Pan for statistical consultation and Dr. M. B. Schaffler, K. D. Burrell, and B. Riemer-McCreadie for technical assistance. This work was supported by National Institutes of Health Grant AR-34399.

References

1. Aitken, J. M. Factors affecting the distribution of zinc in the human skeleton. Calcif Tissue Res 20:23–30; 1976.
2. Amling, M., Herden, S., Posl, M., Hahn, M., Ritzel, H., and Delling, G. Heterogeneity of the skeleton: Comparison of the trabecular microarchitecture of the spine, the iliac crest, the femur, and the calcaneus. J Bone Miner Res 11:36–45; 1996.
3. Amprino, R. Investigations on some physical properties of bone tissue. Acta Anat 34:161–186; 1958.
4. Ascenzi, A., Baschieri, P., and Benvenuti, A. The bending properties of single osteons. J Biomech 23:763–771; 1990.
5. Ascenzi, A., Benvenuti, A., and Bonucci, E. The tensile properties of single osteonic lamellae: Technical problems and preliminary results. J Biomech 15:29–37; 1982.
6. Ascenzi, A. and Bonucci, E. The tensile properties of single osteons. Anat Rec 158:375–386; 1967.
7. Ascenzi, A. and Bonucci, E. The compressive properties of single osteons. Anat Rec 161:377–391; 1968.
8. Ascenzi, A. and Bonucci, E. The shearing properties of single osteons. Anat Rec 172:499–510; 1972.
9. Ascenzi, A., Improta, S., Portigliatti Barbos, M., Carando, S., and Boyde, A. Distribution of lamellae in human femoral shafts deformed by bending with inferences on mechanical properties. Bone 8:319–325; 1987.
10. Ashman, R. B. and Rho, J. Y. Elastic modulus of trabecular bone material. J Biomech 21:177–181; 1988.
11. Baker, P. B. and Weihs, T. P. The analysis of depth-sensing indentation data: Review of the special discussion session. Materials Research Society Symposium Proceedings, Vol. 308; 1993; 217–219.
12. Brown, T. D. and Ferguson, A. B., Jr. Mechanical property distributions in the cancellous bone of the human proximal femur. Acta Orthop Scand 51:429–437; 1980.
13. Burr, D. B., Forwood, M. R., Fyhrie, D. P., Martin, R. B., Schaffler, M. B., and Turner, C. H. Bone microdamage and skeletal fragility in osteoporotic and stress fractures. J Bone Miner Res 12:6–15; 1997.
14. Butler, W. T., Ridall, A. L., and McKee, M. D. Osteopontin. In: Bilzekian, J. P., Raisz, L. G., and Rodan, G. A., Eds. Principles of bone biology. San Diego: Academic Press; 1996.
15. Carlstrom, D. Micro-hardness measurements on single haversian systems in bone. Experientia 10:171–172; 1954.
16. Chalmers, J. Distribution of osteoporotic changes in the ageing skeleton. Clin Endocrinol Metab 2:203–220; 1973.
17. Choi, K. and Goldstein, S. A. A comparison of the fatigue behavior of human trabecular and cortical bone tissue. J Biomech 25:1371–1381; 1992.
18. Choi, K., Kuhn, J. L., Ciarelli, M. J., and Goldstein, S. A. The elastic moduli of human subchondral, trabecular, and cortical bone tissue and the size-dependency of cortical bone modulus. J Biomech 23:1103–1113; 1990.

19. Ciarelli, M. J., Goldstein, S. A., Kuhn, J. L., Cody, D. D., and Brown, M. B. Evaluation of orthogonal mechanical properties and density of human trabecular bone from the major metaphyseal regions with materials testing and computed tomography. J Orthop Res 9:674–682; 1991.
20. Cooper, C. The epidemiology of fragility fractures: Is there a role for bone quality? Calcif Tissue Int 53:S23–S26; 1993.
21. Currey, J. D. and Brear, K. Hardness, Young's modulus and yield stress in mammalian mineralized tissues. J Mater Sci Mater Med 1:14–20; 1990.
22. Doerner, M. F. and Nix, W. D. A method for interpreting the data from depth-sensing indentation instruments. J Mater Res 1:601–609; 1986.
23. Evans, F. G. Mechanical properties and histology of cortical bone from younger and older men. Anat Rec 185:1–11; 1976.
24. Evans, F. G. and Bang, S. Differences and relationships between the physical properties and microscopic structure of human femoral, tibial and fibular cortical bone. Am J Anat 120:79–88; 1967.
25. Evans, G. P., Behiri, J. C., Currey, J. D., and Bonfield, W. Microhardness and Young's modulus in cortical bone exhibiting a wide range of mineral volume fractions, and in a bone analogue. J Mater Sci Mater Med 1:38–43; 1990.
26. Fondrk, M., Bahniuk, E., Davy, D. T., and Michaels, C. Some viscoplastic characteristics of bovine and human cortical bone [see comments]. J Biomech 21:623–630; 1988.
27. Goldstein, S. A. The mechanical properties of trabecular bone: Dependence on anatomic location and function. J Biomech 20:1055–1061; 1987.
28. Goldstein, S. A., Wilson, D. L., Sonstegard, D. A., and Matthews, L. S. The mechanical properties of human tibial trabecular bone as a function of metaphyseal location. J Biomech 16:965–969; 1983.
29. Gong, J. K., Arnold, J. S., and Cohn, S. H. Composition of trabecular and cortical bone. Anat Rec 149:325–332; 1964.
30. Guo, X. E., Zysset, P. K., Hoffler, C. E., Moore, K. E., and Goldstein, S. A. An application of nanoindentation technique to measure bone lamellae properties. J Biomech Eng. In press.
31. Heaney, R. P. Is there a role for bone quality in fragility fractures? Calcif Tissue Int 53:S3–S5; discussion S5–S6; 1993.
32. Hodgskinson, R., Currey, J. D., and Evans, G. P. Hardness, an indicator of the mechanical competence of cancellous bone. J Orthop Res 7:754–758; 1989.
33. Hoffler, C. E., Guo, X. E., Zysset, P. K., Moore, K. E., and Goldstein, S. A. Evaluation of bone microstructural properties: Effect of testing conditions, depth, repetition, time delay and displacement rate. In: Chandran, K. B., Vanderby, R., Jr., and Hefzy, M. S., Eds. Proceedings of the 1997 Bioengineering Conference, Vol. BED-35. Sun River, OR; 1997; 567–568.
34. Ingram, R. T., Clarke, B. L., Fisher, L. W., and Fitzpatrick, L. A. Distribution of noncollagenous proteins in the matrix of adult human bone: Evidence of anatomic and functional heterogeneity. J Bone Miner Res 8:1019–1029; 1993.
35. Katz, J. L. and Meunier, A. Scanning acoustic microscope studies of the elastic properties of osteons and osteon lamellae. J Biomech Eng 115:543–548; 1993.
36. Keaveny, T. M. and Hayes, W. C. A 20-year perspective on the mechanical properties of trabecular bone. J Biomech Eng 115:534–542; 1993.
37. King, R. B. Elastic analysis of some punch problems for a layered medium. Int J Solids Struct 23:1657–1664; 1987.
38. Ko, C.-C., Douglas, W. H., and Cheng, Y. S. Intrinsic mechanical competence of cortical and trabecular bone measured by nanoindentation and microindentation probes. In: Hochmuth, R. M., Langrana, N. A., and Hefzy, M. S., Eds. Bioengineering Conference, ASME, Vol. BED-29. Beaver Creek, CO; 1995; 415–416.
39. Kuhn, J. L., Goldstein, S. A., Choi, K., London, M., Feldkamp, L. A., and Matthews, L. S. Comparison of the trabecular and cortical tissue moduli from human iliac crests. J Orthop Res 7:876–884; 1989.
40. Lips, P. Epidemiology and predictors of fractures associated with osteoporosis. Am J Med 103:3S–8S; 1997.
41. Mbuyi-Muamba, J.-M. and Dequeker, J. Biochemical anatomy of human bone: Comparative study of compact and spongy bone in femur, rib and iliac crest. Acta Anat 128:184–187; 1987.
42. Mente, P. L. and Lewis, J. L. Experimental method for the measurement of the elastic modulus of trabecular bone tissue. J Orthop Res 7:456–461; 1989.
43. Ninomiya, J. T., Tracy, R. P., Calore, J. D., Gendreau, M. A., Kelm, R. J., and Mann, K. G. Heterogeneity of human bone. J Bone Miner Res 5:933–938; 1990.
44. Oliver, W. C. and Pharr, G. M. An improved technique for determining hardness and elastic modulus using local and displacement sensing indentation experiments. J Mater Res 7:1564–1583; 1992.
45. Pope, M. H. and Outwater, J. O. Mechanical properties of bone as a function of position and orientation. J Biomech 7:61–66; 1974.
46. Reilly, D. T. and Burstein, A. H. Review article. The mechanical properties of cortical bone. J Bone Jt Surg Am 56:1001–1022; 1974.
47. Resnick, D. and Niwayama, G. Entheses and enthesopathy. Anatomical, pathological, and radiological correlation. Radiology 146:1–9; 1983.
48. Rho, J. Y., Ashman, R. B., and Turner, C. H. Young's modulus of trabecular and cortical bone material: Ultrasonic and microtensile measurements. J Biomech 26:111–119; 1993.
49. Rho, J. Y., Hobatho, M. C., and Ashman, R. B. Anatomical variation of mechanical properties of human cancellous bone. In: Hochmuth, R. M., Langrana, N. A., and Hefzy, M. S., Eds. Bioengineering Conference, ASME, Vol. BED-29. Beaver Creek, CO; 1995; 365–366.
50. Rho, J. Y., Hobatho, M. C., and Ashman, R. B. Anatomical variation of mechanical properties of human cortical bone. In: Hochmuth, R. M., Langrana, N. A., and Hefzy, M. S., Eds. Bioengineering Conference, ASME, Vol. BED-29. Beaver Creek, CO; 1995; 239–240.
51. Rho, J. Y., Tsui, T. Y., and Pharr, G. M. Elastic properties of human cortical and trabecular lamellar bone measured by nanoindentation. Biomaterials 18: 1325–1330; 1997.
52. Robey, P. G. Bone matrix proteoglycans and glycoproteins. In: Bilzekian, J. P., Raisz, L. G., and Rodan, G. A., Eds. Principles of bone biology. San Diego: Academic Press; 1996; 155–165.
53. Roy, M., Rho, J. Y., Tsui, T. Y., and Pharr, G. M. Variations of Young's modulus and hardness in human lumbar vertebrae measured by nanoindentation. In: Rastegar, S., Ed. Advances in bioengineering, Vol. BED-33. Atlanta, GA: American Society of Mechanical Engineers; 1996; 385–386.
54. Runkle, J. C. and Pugh, J. The micro-mechanics of cancellous bone. II. Determination of the elastic modulus of individual trabeculae by a buckling analysis. Bull Hosp Jt Dis 36:2–10; 1975.
55. Ryan, S. D. and Williams, J. L. Tensile testing of rodlike trabeculae excised from bovine femoral bone. J Biomech 22:351–355; 1989.
56. Shieh, S. J., Govind, S., Gudipaty, K., Subramanian, R., and Grimm, M. J. High resolution ultrasonic measurements of the material properties of cortical and trabecular bone in the human vertebrae. In: Hochmuth, R. M., Langrana, N. A., and Hefzy, M. S., Eds. Bioengineering Conference, ASME, Vol. BED-29. Beaver Creek, CO; 1995; 413–414.
57. Sneddon, I. N. The relation between load and penetration in the axisymmetric boussinesq problem for a punch of arbitrary profile. Int J Eng Sci 3:47–57; 1965.
58. Townsend, P. R., Rose, R. M., and Radin, E. L. Buckling studies of single human trabeculae. J Biomech 8:199–201; 1975.
59. Turner, C. H., Rho, J., Takano, Y., Tsui, T. Y., and Pharr, G. M. The elastic properties of trabecular and cortical bone tissues are similar: Results from two microscopic measurement techniques. J Biomech 32:437–441; 1999.
60. Weaver, J. K. The microscopic hardness of bone. J Bone Jt Surg Am 48:273–288; 1966.
61. Ziv, V., Wagner, H. D., and Weiner, S. Microstructure–microhardness relations in parallel-fibered and lamellar bone. Bone 18:417–428; 1996.
62. Zysset, P. K., Goulet, R. W., and Hollister, S. J. A global relationship between trabecular bone morphology and homogenized elastic properties. J Biomech Eng 120:640–646; 1998.
63. Zysset, P. K., Guo, X. E., Hoffler, C. E., Moore, K. E., and Goldstein, S. A. Elastic modulus and hardness of human cortical and trabecular lamellae measured by nanoindentation. J Biomech 32:1005–1012; 1999.

Date Received: August 5, 1999
Date Revised: December 9, 1999
Date Accepted: December 10, 1999